Strategy for Increasing the Electrode Density of Microelectrode Arrays by Utilizing Bipolar Behavior of a Metallic Film

ARTICLE *in* ANALYTICAL CHEMISTRY · FEBRUARY 2014

Impact Factor: 5.64 · DOI: 10.1021/ac404202p · Source: PubMed

8 AUTHORS, INCLUDING:

Feng Zhu
Peking University
51 PUBLICATIONS **621** CITATIONS
SEE PROFILE

Jiawei Yan
Xiamen University
25 PUBLICATIONS **299** CITATIONS
SEE PROFILE

Irina Svir
Ecole Normale Supérieure de Paris
82 PUBLICATIONS **834** CITATIONS
SEE PROFILE

analytical chemistry

Article

pubs.acs.org/ac

Strategy for Increasing the Electrode Density of Microelectrode Arrays by Utilizing Bipolar Behavior of a Metallic Film

Feng Zhu,[†] Jiawei Yan,*[,†] Shiwei Pang, Yongliang Zhou,[†] Bingwei Mao,[†] Alexander Oleinick,[‡] Irina Svir,[‡] and Christian Amatore*[,‡]

[†]State Key Laboratory for Physical Chemistry of Solid Surfaces, and Department of Chemistry, College of Chemistry and Chemical Engineering, Xiamen University, Xiamen, Fujian 361005, People's Republic of China

[‡]CNRS UMR 8640 "PASTEUR", Departement de Chimie, Ecole Normale Superieure, 24 rue Lhomond, Paris 75005, France

ABSTRACT: Recessed microelectrode arrays and plane-recessed microelectrode arrays (MEAs) with different center-to-center distances are designed and fabricated using lithographic technology. By comparing electrochemical behavior of plane-recessed MEAs with that of recessed MEAs, bipolar phenomenon of the metallic plane film is revealed. Redox cycling can occur when the top plane electrode was floating; that is, the bipolar behavior of the unbiased top plane electrode may perform locally as a collector and enlarge the concentration gradient of $Ru(NH_3)_6Cl_3$ and thus promote an apparent generator/collector electrochemical response of the microdisk electrode in the MEAs configuration. By utilizing the bipolar behavior, the center-to-center distance of MEAs required for achieving steady-state current could decrease without favoring at the same time the overlapping of diffusion layers of microelectrodes, and thus, the electrode density of MEAs can be increased. Therefore, the bipolar behavior of the metallic film can increase both the current response of an individual microdisk and the electrode density of microdisks without losing the characteristics of a microelectrode. By just fabricating a thin layer of metallic film on the plane and leaving it floating without potential control, recessed MEAs used in this work can achieve the increase of detection sensitivity by more than 1 order of magnitude.

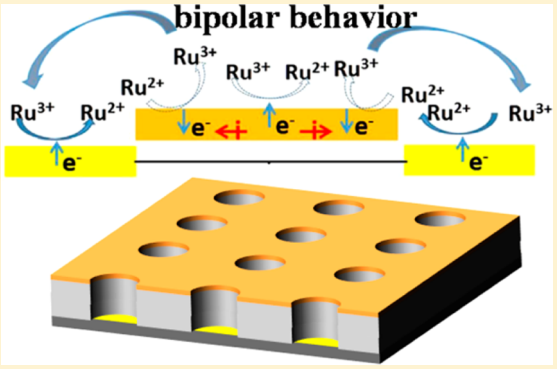

The microelectrode attracts intense attention due to the radial diffusion arising from its small size in at least one dimension. It exhibits the advantages of high current density, fast response time, reduced charging current, small time constant, and high signal-to-noise ratio.[1,2] However, the small output signal of the microelectrode may restrict its application. Microelectrode arrays (MEAs), as a collection of microelectrodes, overcome the disadvantage of low current response of a single microelectrode. MEAs have been widely used in electrochemical detection,[3−9] and continuous efforts have been devoted to improve detection performance, including optimization of geometry of MEAs,[10,11] design and fabrication of functional MEAs with a double-electrode system,[12−15] preparation of a nanoscale electrode array,[16] and integration with a microfluidic or nanochannel chip.[17−20] The center-to-center distance, d, between neighboring microelectrodes in MEAs is a key factor since it significantly affects the electrochemical response of the device. When the d value with respect to that of the active size of each microelectrode is sufficiently large, individual diffusion layers do not overlap. Hence, a steady-state condition could be attained with a total signal that is simply the sum of the signals from individual microelectrodes, i.e., the total signal can be expressed by Ni_{ss}, where N is the number of microelectrodes and i_{ss} is the steady-state current of each microelectrode. In contrast, when d is too small, the response of the MEAs loses the steady-state characteristic because the overlapping of diffusion layers leads to the development of a planar diffusion wave. Therefore, it is important to seek for the smallest value of d in order to prevent the overlapping of diffusion layers of microelectrodes and thus accommodate microelectrodes with highest density for higher detection sensitivity.

Theoretical studies have been continuously performed for investigating the shortest distance with steady-state response. Different values of d had ever been proposed to achieve an independent diffusion layer.[21,22] And it was revealed by Amatore et al. that, regardless of the size of d, there would be coupling between neighboring individual microelectrodes at slow scan rate since the diffusion layer develops with time.[23] Then Compton and co-workers proposed a formula of $d > 2\sqrt{2D\Delta E/\nu}$ to estimate the distance because the diffusion layer is related with the time period and diffusion coefficient (ΔE is the width of the potential scan, and ν is the scan rate).[24,25] Recently, Guo and Lindner showed some diffusion modes and drew a zone diagram of cyclic voltammetric behavior of MEAs by introducing dimensionless parameters and concluded that

Received: December 26, 2013
Accepted: February 14, 2014
Published: February 14, 2014

   dx.doi.org/10.1021/ac404202p | *Anal. Chem.* 2014, 86, 3138−3145

the relationship satisfying individual diffusion layer would be $d > 23r$ at a certain scan rate range, where r is the radius of the microelectrode.[26] For recessed MEAs, the shortest d for keeping an individual diffusion layer is a little smaller than that of the corresponding inlaid MEAs because act of diffusion layers are confined in the cavity. The inlaid MEAs zone diagram was extended to the recessed MEAs, and a formula to predict the necessary d for steady-state behavior was proposed.[26] Some of us presented numerical simulation of recessed MEAs and evaluated the dependence of the diffusion process on the main geometry, d, and slope of side walls of conical recesses.[27]

Experimental investigations are also carried out to reveal the relationship between v, r, d, and cyclic voltammetric response. By designing a series of MEAs, Sandison et al.[28] validated that the voltammetric behavior of MEAs with constant individual microelectrode radius varies obviously with different d, the larger the d, the more sigmoidal the voltammogram behaves, which is consistent with what theory expected. Furthermore, at fixed relative d/r values, the behavior of MEAs differs greatly with different individual microelectrode radii, and the MEAs with the smallest individual radius produce a strongly peak-shaped voltammogram due to the above revealed by Amatore, Compton, and Lindner. Rahman and Guiseppi-Elie[29] made a detailed investigation by combining digital simulation with experiments to evaluate design optimization for using MEAs in implantable biosensors. And they proposed that the balance between the overall device footprint and the steady-state response from the noninteracting microdisk is the most important criteria.

The above demonstrate that understanding the behaviors of MEAs and improving their performance is a long-term goal and depends on the operative condition. However, the feature of inherent diffusion restricts the electrode density of MEAs. Therefore, it is still a challenging task to break through the limitation of inherent diffusion and thus obtain higher steady-state response without changing chip area by a simple and feasible method. Furthermore, in addition to all the above works which are based on pure diffusional condition, the role of natural convection needs also to be considered when d and r are not very small versus the thickness of the convection free layer.[30]

In recent years, bipolar systems were introduced in electrochemical detection devices since they present attractive features. The bipolar behavior of a conducting object may originate from high voltage when the conducting object is immersed in a solution exposed to an external electric field. It can be categorized as a high electric field induced bipolar phenomenon. On the basis of the bipolar behavior, selective surface modification in the micro- and nanoscale, concentrating, separating, and detecting platform are established.[31−35]

Besides the high electric field induced bipolar phenomenon, the bipolar behaviors can also be observed under some circumstances without the existence of an external electric field. For example, the positive feedback mode in scanning electrochemical microscopy (SECM) technique can be performed at unbiased conducting substrate when the substrate area is much larger than the tip size.[36,37] The phenomenon can be ascribed to concentration gradient induced bipolar behavior. In 2011, Some of us[38] as well as Battistel and Daniele pointed out that, when the probed substrate is not much larger than the size of tip, the bipolar behavior at unbiased substrates will be greatly limited, which is generally overlooked in most SECM experimental investigations and may lead to misinterpreted data. In the field of MEAs, the Niwa group observed the amplification of limiting current that resulted from positive feedback on a micro−macro twin electrode system when the macroelectrode surface area is much larger than that of the microelectrode. This phenomenon was used to detect electroactive compounds.[39−41]

In our previous work about selective detection based on interference depleting and redox cycling using MEAs, we found that the steady-state current of $Ru(NH_3)_6Cl_3$ in generator/collector mode was just a little larger than that in generator/floating-collector mode.[8] In a following work, we validated by simulation methods that redox cycling can occur when the top plane electrode was floating; that is, the bipolar behavior of unbiased top plane electrode may perform locally as a collector and enlarge the concentration gradient of $Ru(NH_3)_6Cl_3$ and thus promote an apparent generator/collector electrochemical response of the microdisk electrode in the MEAs configuration.[42] Figure 1a shows a sketch of the array, which is composed of a top plane electrode and an array of microcavities. The Au microdisk electrodes are located at the bottom of the cylindrical microcavities. The bipolar behavior of an unbiased top plane electrode in each device is depicted in Figure 1b. When the reductive reaction occurs at the recessed disks of the MEA, the upper plane edge near the entrance of each well senses the concentration gradient and induces a reverse reaction, thus acting as an anode (i.e., generating Ru(III) by oxidizing the Ru(II) formed at the recessed disk). In order to maintain the neutrality of the plane Au film, the ensuing oxidation current is compensated at other locations (near the centers between wells) of the top plane Au film which perform as a series of cathodes. Therefore, the concentration gradient of Ru(III) increases, which results in an enhancement in current leading to an overall behavior similar to that observed when the same device is operated as a generator/collector mode (i.e., when the top plane potential is posed at the plateau of the Ru(II) oxidation wave).[8] On the basis of the above, the fact that bipolar behavior of a floating electrode can influence concentration gradient of microelectrodes presents an opportunity to control the spacial status of diffusion layers of microelectrodes, hence allowing higher electrode density.

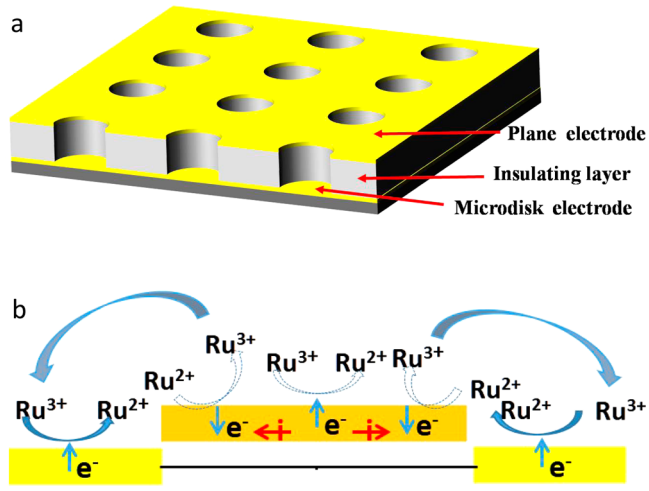

Figure 1. (a) Sketch of the plane-recessed microdisk electrodes array microfabricated and used in this work. (b) Schematic illustration of bipolar behavior of the plane Au film occurring in the plane-recessed MEAs.

dx.doi.org/10.1021/ac404202p | Anal. Chem. 2014, 86, 3138−3145

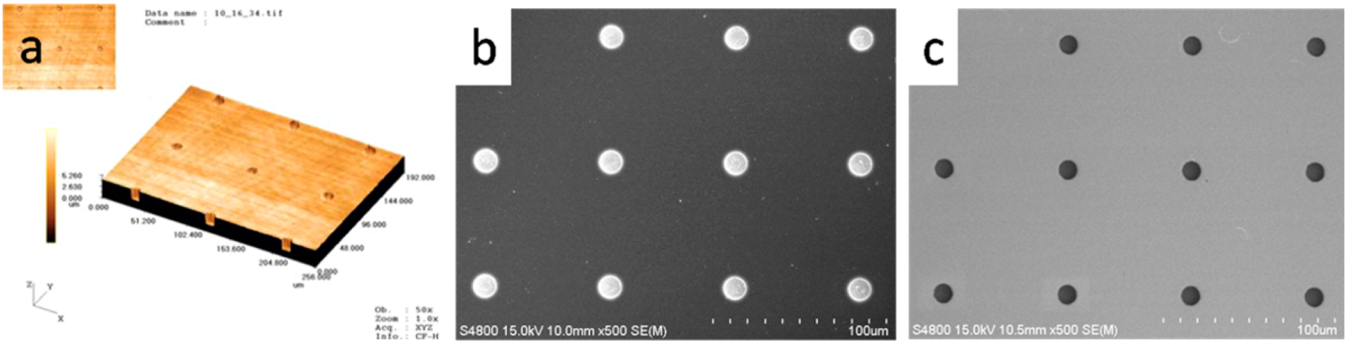

Figure 2. (a) Confocal optical microscopy image of plane-recessed MEAs. (b) SEM image of recessed MEAs. (c) SEM image of plane-recessed MEAs.

In this work, we fabricated a series of recessed MEAs and plane-recessed MEAs with different center-to-center distances using lithographic technology. By comparing recessed MEAs with plane-recessed MEAs, the influence of bipolar behaviors of the floating plane electrode on the diffusion layer and electrochemical response were investigated systematically. These results have then been used for optimizing the bipolar behavior for improving the performance of MEAs.

EXPERIMENTAL SECTION

Materials and Reagents. All chemicals were used as received. Aqueous solutions were prepared using fresh ultrapure Milli-Q water with resistivity of 18.2 MΩ·cm. $Ru(NH_3)_6Cl_3$ was purchased from Sigma-Aldrich; KNO_3, HNO_3, CH_3COOH, H_3PO_4, I_2, KI, $Ce(NH_4)_2(NO_3)_6$, and $HClO_4$ obtained from Sinopharm Chemical Reagents Co. were of analytical grade. Agar was obtained from Quanzhou City Quangang chemical plant.

Electrodes. Two types of microelectrode arrays (MEAs) were microfabricated: conducting top plane recessed disk microelectrode arrays (plane-recessed MEAs) and recessed microelectrode arrays into an insulating layer (recessed MEAs). For each type, seven kinds of arrays were microfabricated with different center−center distances while keeping constant the radius of the microelectrode, i.e., $d \sim 3r$, $d \sim 6r$, $d \sim 8r$, $d \sim 10r$, $d \sim 12r$, $d \sim 15r$, and $d \sim 20r$. The area of the plane electrode of plane-recessed MEAs was fixed as 2×2 mm^2.

The microfabrication procedure for plane-recessed MEAs was described elsewhere in detail.[8] Briefly, a layer of thermal oxide was grown on 4 in. diameter silicon wafer. Next, a layer of Cr/Au was sputtered on the wafer and patterned through a first mask, and the exposed Au was etched by KI/I_2 etchant. Following, a chromium etchant consisting of a mixture of $Ce(NH_4)_2(NO_3)_6$ and $HClO_4$ was used to etch the underlying Cr film. Then a layer of polyimide precursor was spin-coated onto the wafer and cured, and the polyimide layer served as insulating layer to separate the next-to-be top plane electrode and microdisk electrodes. After that, another layer of Cr/Au was patterned through lift-off by using a second mask perfectly aligned with the second microdisk array. The patterned Cr/Au layer functions as mask to etch exposed polyimide using inductively coupled plasma (ICP) etching. In order to microfabricate recessed MEAs, the sputtering of the second Cr/Au layer was replaced by Al evaporation. Accordingly, the Al layer was used as a mask in the process of ICP etching. After the definition of the microdisk electrode and contact pad, the Al layer was removed through wet etching with a mixture of $HNO_3/CH_3COOH/H_2O/H_3PO_4$.

The morphologies of plane-recessed MEAs and recessed MEAs were characterized by confocal microscopy (OLS1200, Olympus) and scanning electronic microscopy (SEM) (Hitachi S-4800). The recess depth of the MEAs was probed using a profilometer (Dekta 3, Veeco).

Electrochemical Experiments. All electrochemical experiments were carried out on a CHI814A (Chenhua Corp., China) or an Autolab (PGSTAT128N, Metrohm) electrochemical workstation. MEAs were electrochemically cleaned by potential scans between 0.2 and 1.4 V in 0.1 M H_2SO_4 prior to electrochemical measurements. For recessed MEAs, a conventional three-electrode system was adopted, with recessed MEAs as interconnected working electrodes, a large Au foil as counter electrode, and a saturated calomel electrode (SCE) as reference electrode bridged through KNO_3 saturated agar gel. For plane-recessed MEAs operated in single mode (i.e., when the plane electrode is floating), the same configuration as that of recessed MEAs was adopted. For plane-recessed MEAs operated in dual mode (i.e., when the plane electrode is connected), the electrode potentials of the plane electrode and the recessed MEAs were controlled independently with respect to the reference electrode; the plane electrode was held at 0.05 V while the recessed MEAs were swept from 0.05 to −0.4 V.

RESULTS AND DISCUSSION

Physical Characterization of the MEAs. Confocal microscopy was used to obtain a three-dimensional (3D) optical image of the MEAs. As shown in Figure 2a, we can clearly observe the ordered arrangement of microdisk electrodes, which are located at the bottom of the microcavities. The diameter of individual microelectrode was measured by SEM. SEM images of plane-recessed MEAs and recessed MEAs are shown in Figure 2, parts b and c, respectively. Both images demonstrate a quadratic arrangement of the microdisk electrodes, which is consistent with the result of confocal microscopy and reveals that the diameters of the microdisk electrodes of both plane-recessed MEAs and recessed MEAs are 12.0 ± 0.5 μm. The depth of the microcavities was characterized using a profilometer. It is about 2.0 μm for plane-recessed MEAs. For recessed MEAs, the depth was about 2.4 μm, while the thickness of Al film was 0.3 μm before the Al film was etched. The wet etching of the Al film in etchant may result in a partial shrinking of the polyimide layer. The thickness of the insulating layer, viz., the insulating length of the microwell's walls, was designed to ensure the overlapping of

dx.doi.org/10.1021/ac404202p | Anal. Chem. 2014, 86, 3138−3145

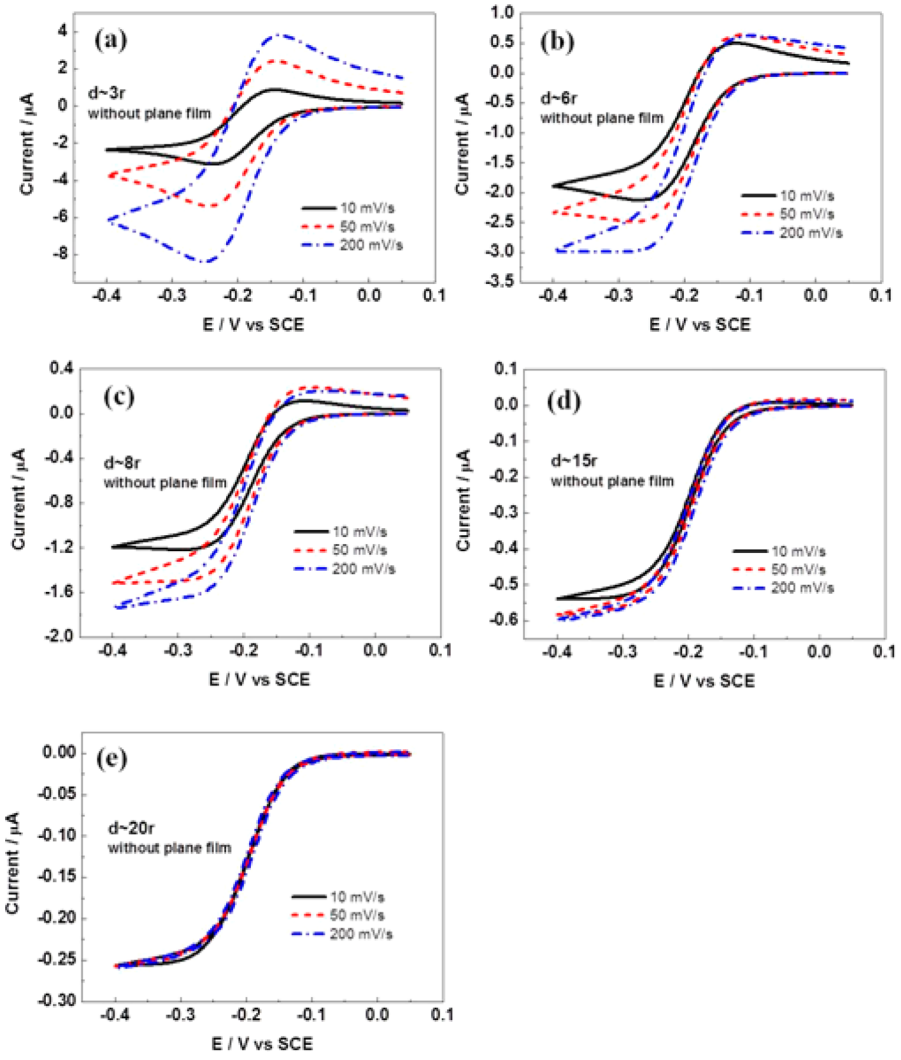

Figure 3. Electrochemical responses of recessed MEAs with different interelectrode distances at various scan rates. Solution: 5 mM $Ru(NH_3)_6Cl_3$ + 0.5 M KNO_3.

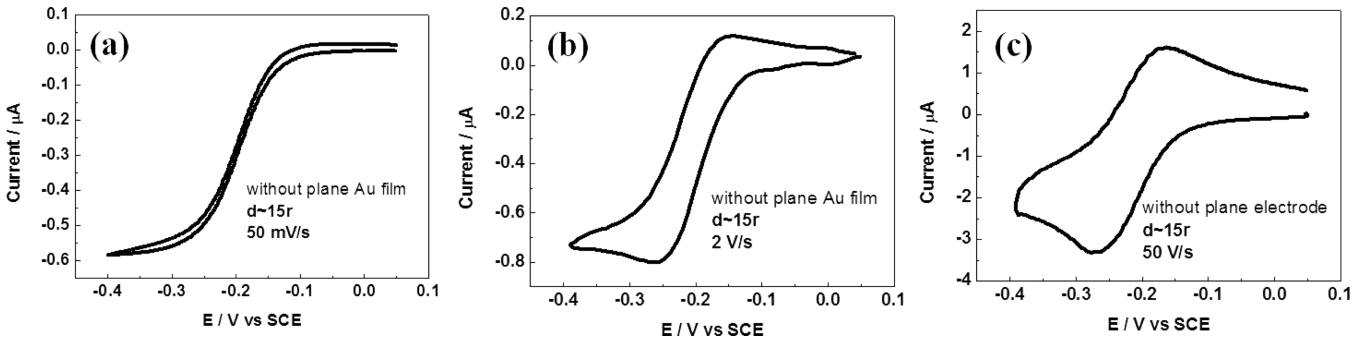

Figure 4. Cyclic voltammograms of recessed MEA with $d \sim 15r$. Scan rate: (a) 50 mV/s, (b) 2 V/s, and (c) 50 V/s. Solution: 5 mM $Ru(NH_3)_6Cl_3$ + 0.5 M KNO_3.

diffusion layers between the plane electrode and microdisk electrodes, which is an important factor to induce the occurrence of bipolar behavior.[42]

Electrochemical Investigation of the Recessed MEAs. Without a conducting top plane, the normal characteristic of the recessed MEAs could be recorded without any involvement of bipolar phenomena. First, we investigated the electrochemical behaviors of the recessed MEAs by measuring voltammetric responses for different d/r ratios and different scan rates; this helped to experimentally determine the shortest d/r for recording a pure steady-state behavior. Cyclic voltammograms (CVs) of the recessed MEAs in 5 mM $Ru(NH_3)_6Cl_3$ are shown in Figure 3. It can be seen that when d equals to $3r$ (Figure 3a), the CV presents peak-shaped characteristic, indicating consequent overlapping of diffusion layers of the adjacent microelectrodes. Upon increasing d/r,

dx.doi.org/10.1021/ac404202p | Anal. Chem. 2014, 86, 3138−3145

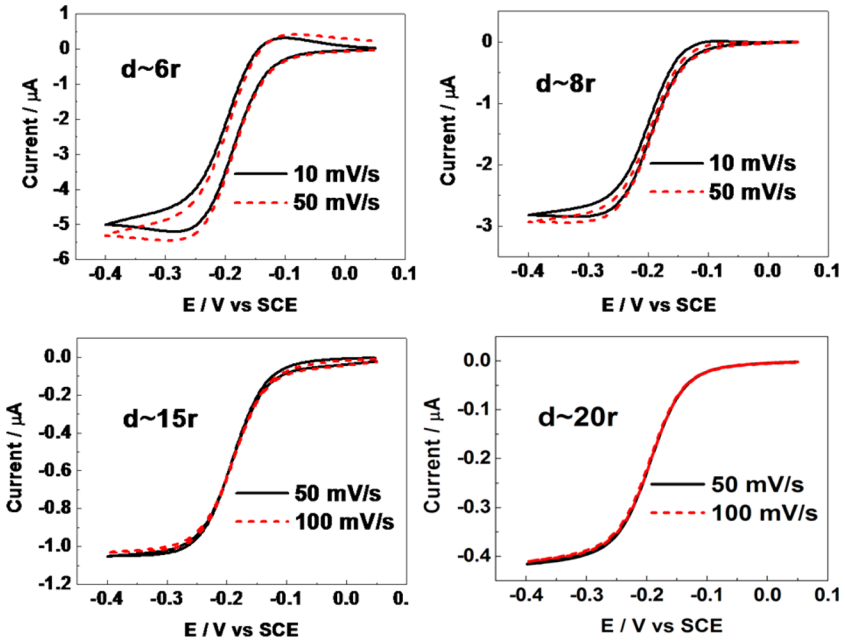

Figure 5. Cyclic voltammograms of plane-recessed MEAs with different interelectrode distances when the plane electrode was floating. Solution: 5 mM $Ru(NH_3)_6Cl_3$ + 0.5 M KNO_3.

Table 1. Experimental Data for Recessed MEAs and Plane-Recessed MEAs at Single Mode[a]

d	N	area (10^{-9} m^2)	current intensity (A) (exptl data, recessed MEAs, 10 mV/s)	current density of recessed MEA (μA/mm^2)	current intensity (A) (exptl data, plane-recessed MEA)	current density of plane-recessed MEA (μA/mm^2)
3r	1936	218.8	-3.13×10^{-6} (p)			
6r	484	54.7	-1.93×10^{-6} (p−s)	35.3	-5.20×10^{-6} (p−s)	95.1
8r	256	28.9	-1.23×10^{-6} (p−s)	42.6	-2.90×10^{-6} (ss)	100.0
10r	144	16.3	-8.2×10^{-7} (p−s)	50.3	-1.80×10^{-6} (ss)	110.4
12r	100	11.3	-6.4×10^{-7} (p−s)	56.7	-1.23×10^{-6} (ss)	109.0
15r	81	9.2	-5.5×10^{-7} (p−s)	57.6	-1.00×10^{-6} (ss)	109.0
20r	36	4.1	-2.4×10^{-7} (ss)	61.0	-4.0×10^{-7} (ss)	97.6

[a]"N" represents the number of recessed microdisk electrodes; area is the calculated surface area of microdisks only; "p" indicates planar diffusion controlled, and the reduction peak current is read; "p−s" indicates the mixed diffusion mode, and current at −0.3 V is read when potential was scanned negatively; "ss" indicates steady-state, and cathodic limiting plateau current is taken. Current density is normalized by relative area and expressed in terms of positive values.

current responses gradually shifted from peak-shaped to sigmoidal wave. When d was equal to 15r (Figure 3d), electrochemical behavior of recessed MEAs approaches steady state at the lower scan rates. Conversely at $d \sim 20r$ (Figure 3e), the CVs of recessed MEAs remained unchanged when the scan rate was varied from 10 to 200 mV/s and exhibited perfect steady-state characteristic. Therefore, it could be concluded that, under our measured conditions of analytical interest, the shortest d to avoiding the overlapping of diffusion layers should be between 15r and 20r for the MEAs configuration used in this work.

However, increasing the scan rate beyond the range investigated in Figure 3, cyclic voltammograms corresponding to other diffusion modes are observed as shown in Figure 4. For a scan rate of 50 mV/s, the MEAs present a sigmoidal curve (Figure 4a), which is a symbol of radial diffusion process (i.e., diffusion layers of individual electrodes do not overlap). When a high scan rate of 50 V/s is applied, the cyclic voltammogram features obvious anodic and cathodic peak current (Figure 4c), which is characteristic of planar diffusion at an individual microelectrode. For a moderate scan rate of 2 V/s, a transitional state between radial diffusion and transition stage is observed as shown in Figure 4b.

The above experiments not only reveal the electrochemical behaviors of the recessed MEAs including the shortest d to avoiding the overlapping of diffusion layers but also serve as controls for assuring and understanding bipolar effects due to the presence of the top plane electrode in plane-recessed MEAs.

Electrochemical Investigation at Plane-Recessed MEAs. In order to investigate the electrochemical behavior of plane-recessed MEAs, the top plane electrode could be floating or held at a constant potential while microdisk electrodes are swept from 0.05 to −0.4 V to monitor the reductive current of $Ru(NH_3)_6Cl_3$. The two cases are named as single mode and dual or generator (microdisk)/collector (plane) mode, respectively. And the two modes are investigated separately in the following.

Single Mode: The Effect of Bipolar Behavior of the Plane Electrode. At single mode, cyclic voltammograms of the plane-recessed MEAs with different interelectrode distances were measured, and typical results are shown in Figure 5. It can be seen that, even when the upper plane Au electrode is left

dx.doi.org/10.1021/ac404202p | Anal. Chem. 2014, 86, 3138−3145

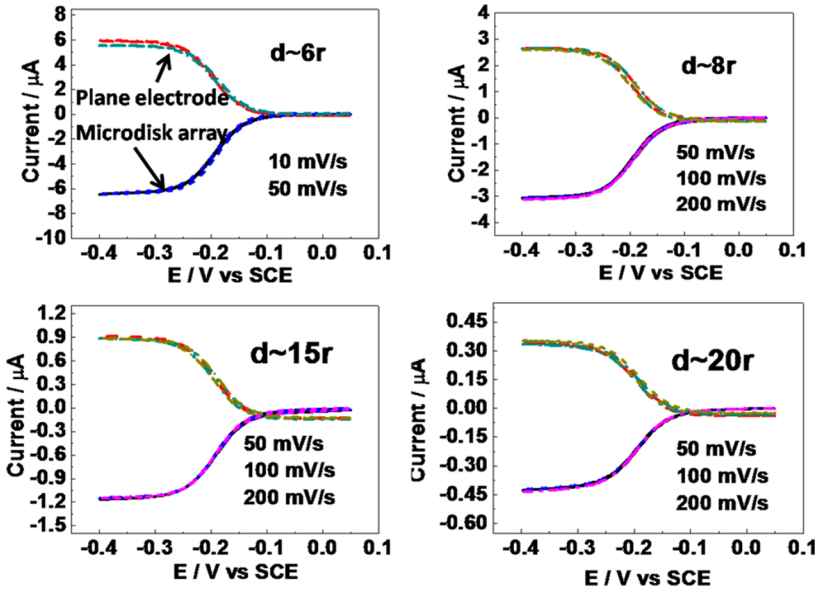

Figure 6. Electrochemical responses of plane-recessed MEAs with different interelectrode distances working in generator/collector mode. The microdisk array was swept at various sweep rates while the plane electrode was held at 0.05 V. Solution: 5 mM $Ru(NH_3)_6Cl_3$ + 0.5 M KNO_3.

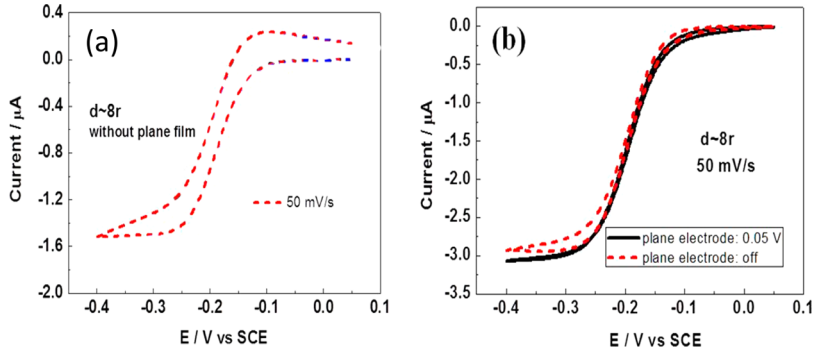

Figure 7. (a) Electrochemical response of recessed MEAs. (b) Electrochemical response of plane-recessed MEAs when the plane electrode is floating (dashed line) or held at 0.05 V (solid line). Solution: 5 mM $Ru(NH_3)_6Cl_3$ + 0.5 M KNO_3.

unconnected, the changes of electrochemical responses with increasing d are remarkably different from those observed above for recessed MEAs. For example, even at rather small d/r values (Figure 5 top) an increase of scan rate from 10 to 50 mV/s results in a very moderate trend toward non-steady-state behavior in drastic contrast with what was observed in Figure 3a−c. More precisely, for $d \sim 6r$, when scan rate increases, the limiting current only increases by around 3%, which is much smaller than the value of around 30% for the recessed MEAs (Figure 3b). Hence, the shortest d for observing steady-state behavior at plane-recessed MEAs ranges between $6r$ and $8r$ for the configuration used in this work. This is evidence that the density of microwells may be increased about 4 times compared to plane-recessed MEAs.

Table 1 contains a summary of experimental data for recessed MEAs and plane-recessed MEAs in single mode. It can be seen that the change tendency of current density of recessed MEAs (column 5 of Table 1) is totally different from that of plane-recessed MEAs (column 7 of Table 1). For recessed MEAs, current density increases gradually as d increases from $3r$ to $20r$ because diffusion layers of individual microdisk electrodes tend to stop overlapping at a center-to-center distance of about $20r$. By contrast, when d is larger than $6r$ for plane-recessed MEAs, electrochemical responses at single mode are steady state as mentioned above. Table 1 shows that current densities are almost identical with an average value of -104.0 ± 6.4 $\mu A/mm^2$, which indicates that, in the presence of upper Au film, the profile of diffusion layers is essentially controlled by the redox cross-talk in each microwell between the disk electrode and the circular edge of the top plane one performing in bipolar mode.

Compared with the steady current at $d \sim 20r$ of recessed MEAs, the steady current at $d \sim 8r$ of plane-recessed MEAs increases by more than 1 order of magnitude owing to the existence of upper Au film, which is a great advantage for detection.

Generator/Collector Mode: Further Evidence for Bipolar Phenomenon. In order to further verify the function of the plane Au film, we investigated the electrochemical behaviors of the plane-recessed MEAs in generator/collector working mode. In 0.5 M KNO_3 solution containing 5 mM $Ru(NH_3)_6Cl_3$, the potential of the plane electrode was held at 0.05 V, which is positive enough to oxidize Ru(II) generated at recessed microdisk electrodes back to its original state Ru(III). The results are shown in Figure 6. At all d ($6-20r$), the collection efficiency[10] of plane electrode to recessed microdisk electrode reaches about 90%. Compared with the electrochemical behaviors of the plane-recessed MEAs in single mode and the

dx.doi.org/10.1021/ac404202p | *Anal. Chem.* 2014, 86, 3138−3145

recessed MEAs, the current signals in generator/collector mode are quite similar with those in single mode, and much different from those for recessed MEAs (see Figure 7 which takes $d \sim 8r$ as example). The above demonstrate that, even in single mode, redox cycling occurs between the plane electrode and the recessed microdisk electrode array; that is, the floating Au top plane film develops a bipolar potential distribution.[42] This is sufficient to induce a significant rate of electrochemical reaction at the plane edge as described schematically in Figure 1b. When the reduction occurs at the plane-recessed MEAs, the upper plane near the entrance of each microwell senses the concentration gradient which is sufficient to induce the reverse reaction, thus acting as a collecting anode, i.e., generating Ru(III) by oxidizing Ru(II) formed at the recessed microdisks. In order to maintain the neutrality of the plane Au film, the ensuing oxidation current is compensated by the part of the floating plane Au film near the center between microwells, which works as a cathode. Therefore, the concentration gradient of Ru(III) increases and results in an enhancement current. Such a redox cycling between disk and plane electrodes in plane-recessed MEAs significantly decreases the diffusion layer vis-à-vis recessed MEAs as schematized in Figure 8. This evidently leads to a smaller diffusion layer overlap in the case of plane-recessed MEAs and hence to a more dense electrode arrangement.

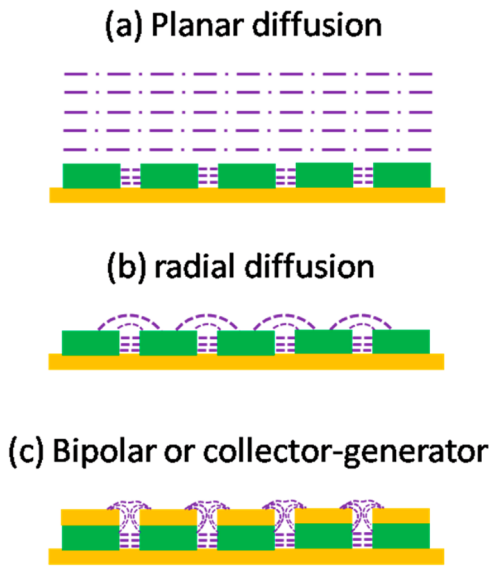

Figure 8. Schematic diagram of diffusion mode for densely packed recessed MEAs at low (a) or faster (b) scan rates. Panel c shows the collector/generator behavior operating when the top plane is conducting; either it is connected (collector/generator mode) or floating (bipolar effect).

The plot of steady-state current of plane-recessed MEAs with different interelectrode distances against number of microelectrodes is shown in Figure 9. It can be seen that, when the plane electrode is held at 0.05 V, the slope value is -1.3×10^{-8} A, which represents an average value of an individual microelectrode. On the other hand, steady-state current for an individual recessed microelectrode can be estimated using the following formula.[43,44]

$$i_{ss} = 4nFC^{b}Dr\frac{\pi r}{4l + \pi r}$$

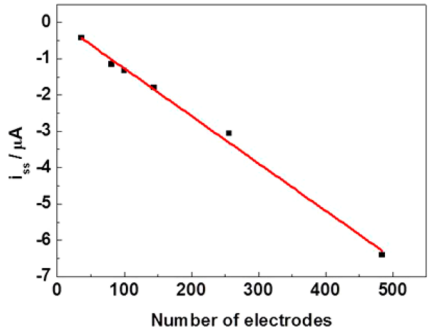

Figure 9. Plot of steady-state current of plane-recessed MEAs with different interelectrode distances against the number of microdisks. The plane electrode was held at 0.05 V. Solution: 5 mM $Ru(NH_3)_6Cl_3$ + 0.5 M KNO_3.

where n is the moles of electrons per mole of analyte, F is the Faraday constant (96 485.31 C/mol), D is the diffusion coefficient (5.32×10^{-6} cm^2/s in 0.5 M KNO_3),[45] C^b is the bulk concentration, r is the radius of the microdisk, and l is the recess height. The calculated value is 4.3×10^{-9} A ($r = 6$ μm, $l = 2$ μm). By comparing the above two values, it can be inferred that the number of redox cycles[11] is approximately 3.0. In the case of the presence of the Au plane film, the response of the microdisk array when the plane film is floating is almost the same as that of the microdisk array when the potential of the plane film was held at 0.05 V. Therefore, a conclusion can be drawn that bipolar behavior of the plane Au film can lead to the increase of current response by about 3 times for each microdisk electrode when $d > 6r$, which is the result of the steeper concentration gradient increased by the top plane edge. This is evidence that the bipolar behavior of a metallic film can be used to increase not only the electrode density of microdisks in an analytical detector but also the current response of an individual microdisk. In view of the effect of multiplying the above two factors together, the presence of a thin layer of metallic film on the plane without controlling its potential increases the performance of a recessed MEA by more than 1 order of magnitude.

CONCLUSIONS

A series of plane-recessed MEAs and recessed MEAs with different center-to-center distances are fabricated, and their electrochemical behaviors are investigated. By comparing the electrochemical behavior of plane-recessed MEAs with that of recessed MEAs, the bipolar phenomenon of the metallic plane film and its function of altering the diffusion profile of the microdisk electrode are revealed. The bipolar behavior of the metallic film can increase both the current response of an individual microdisk and the electrode density of microdisks without losing the characteristics of a microelectrode array. Therefore, the bipolar behavior may be crucial to the integration level of the wafer. By just fabricating a thin layer of metallic film on the plane and leaving it floating without potential control, recessed MEAs can achieve the increase of detection sensitivity by more than 1 order of magnitude. Decreasing the electron-transfer (ET) rate constant will shift more and more each half-wave (viz., the cathodic and anodic contributions) from the couple E. As a consequence, the ensuing current in floating mode will decay drastically since its value features the equal cathodic and anodic currents ones. However, then it is sufficient to operate the system by poising

dx.doi.org/10.1021/ac404202p | Anal. Chem. 2014, 86, 3138−3145

the top plane electrode. So the largest constraint for operating this device with success is not the ET rate constants but the high degree of chemical reversibility of the analyte wave, as opposed to the chemical irreversibility of the interference waves when an interference is present (see our previous works in refs 8, 9, and 42). Only such relative chemical reversibility will lead to the enhancement of the analyte current and virtual annihilation of the interference one due to the occurrence of a positive (analyte) or negative (interference) feedback loop. The feasible strategy of employing the bipolar behavior of a plane metallic film is appealing not only in the field of MEAs but also in other aspects, such as electrochemical microsystems.

AUTHOR INFORMATION

Corresponding Authors

*E-mail: jwyan@xmu.edu.cn.
*E-mail: christian. amatore@ens.fr.

Notes

The authors declare no competing financial interest.

ACKNOWLEDGMENTS

In Xiamen, this work was supported by the Natural Science Foundation of China (Nos. 21373174, 20973144, 21321062), the Natural Science Foundation of Fujian Province of China (No. 2012J01054), the Fundamental Research Funds for the Central Universities (No. 2012121026), and the China Scholarship Council. In Paris, this work was supported in parts by ENS, UPMC, CNRS (UMR 8640) as well as by the ANR (ANR-10-CEXC-012-01 Grant) awarded to I.S. Both groups also thank the CNRS−ENS−Xiamen University international joint laboratory LIA XiamENS for support.

REFERENCES

(1) Dayton, M. A.; Brown, J. C.; Stutts, K. J.; Wightman, R. M. *Anal. Chem.* **1980**, *52*, 946−950.
(2) Wightman, R. M. *Anal. Chem.* **1981**, *53*, 1125A−1134A.
(3) Hood, S. J.; Kampouris, D. K.; Kadara, R. O.; Jenkinson, N.; del Campo, F. J.; Munoz, F. X.; Banks, C. E. *Analyst* **2009**, *134*, 2301−2305.
(4) Gonzalez-Garcia, O.; Arino, C.; Diaz-Cruz, J. M.; Esteban, M. *Sens. Actuators, B* **2008**, *135*, 381−387.
(5) Xie, X. D.; Berner, Z.; Albers, J.; Stuben, D. *Microchim. Acta* **2005**, *150*, 137−145.
(6) Simm, A. O.; Banks, C. E.; Ward-Jones, S.; Davies, T. J.; Lawrence, N. S.; Jones, T. G. J.; Jiang, L.; Compton, R. G. *Analyst* **2005**, *130*, 1303−1311.
(7) Watanabe, T.; Einaga, Y. *Biosens. Bioelectron.* **2009**, *24*, 2684−2689.
(8) Zhu, F.; Yan, J.; Lu, M.; Zhou, Y.; Yang, Y.; Mao, B. *Electrochim. Acta* **2011**, *56*, 8101−8107.
(9) Pang, S. W.; Yan, J. W.; Zhu, F.; He, D. W.; Mao, B. W.; Oleinick, A.; Svir, I.; Amatore, C. *Electrochem. Commun.* **2014**, *38*, 61−64.
(10) Bard, A. J.; Crayston, J. A.; Kittlesen, G. P.; Varco Shea, T.; Wrighton, M. S. *Anal. Chem.* **1986**, *58*, 2321−2331.
(11) Niwa, O.; Morita, M.; Tabei, H. *Anal. Chem.* **1990**, *62*, 447−452.
(12) Huang, X. J.; O'Mahony, A. M.; Compton, R. G. *Small* **2009**, *5*, 776−788.
(13) Barnes, E. O.; Lewis, G. E. M.; Dale, S. E. C.; Marken, F.; Compton, R. G. *Analyst* **2012**, *137*, 1068−1081.
(14) Dam, V. A. T.; Olthuis, W.; van den Berg, A. *Analyst* **2007**, *132*, 365−370.
(15) Barnes, E. O.; Lewis, G. E. M.; Dale, S. E. C.; Marken, F.; Compton, R. G. *J. Electroanal. Chem.* **2013**, *703*, 38−44.
(16) Ma, C.; Contento, N. M.; Gibson, L. R.; Bohn, P. W. *ACS Nano* **2013**, *7*, 5483−5490.
(17) Kätelhön, E.; Hofmann, B.; Lemay, S. G.; Zevenbergen, M. A. G.; Offenhäusser, A.; Wolfrum, B. *Anal. Chem.* **2010**, *82*, 8502−8509.
(18) Goluch, E. D.; Wolfrum, B.; Singh, P. S.; Zevenbergen, M. A. G.; Lemay, S. G. *Anal. Bioanal. Chem.* **2009**, *394*, 447−456.
(19) Wolfrum, B.; Zevenbergen, M.; Lemay, S. *Anal. Chem.* **2008**, *80*, 972−977.
(20) Ma, C.; Contento, N. M.; Gibson, L. R.; Bohn, P. W. *Anal. Chem.* **2013**, *85*, 9882−9888.
(21) Saito, Y. *Rev. Polarogr.* **1968**, *15*, 177−187.
(22) Fletcher, S.; Horne, M. D. *Electrochem. Commun.* **1999**, *1*, 502−512.
(23) Amatore, C.; Savéant, J. M.; Tessier, D. *J. Electroanal. Chem. Interfacial Electrochem.* **1983**, *147*, 39−51.
(24) Davies, T. J.; Ward-Jones, S.; Banks, C. E.; del Campo, J.; Mas, R.; Munoz, F. X.; Compton, R. G. *J. Electroanal. Chem.* **2005**, *585*, 51−62.
(25) Davies, T. J.; Compton, R. G. *J. Electroanal. Chem.* **2005**, *585*, 63−82.
(26) Guo, J. D.; Lindner, E. *Anal. Chem.* **2009**, *81*, 130−138.
(27) Amatore, C.; Oleinick, A. I.; Svir, I. *Anal. Chem.* **2009**, *81*, 4397−4405.
(28) Sandison, M. E.; Anicet, N.; Glidle, A.; Cooper, J. M. *Anal. Chem.* **2002**, *74*, 5717−5725.
(29) Rahman, A.; Guiseppi-Elie, A. *Biomed. Microdevices* **2009**, *11*, 701−710.
(30) Amatore, C.; Pebay, C.; Sella, C.; Thouin, L. *ChemPhysChem* **2012**, *13*, 1562−1568.
(31) Loget, G.; Kuhn, A. *Anal. Bioanal. Chem.* **2011**, *400*, 1691−1704.
(32) Ulrich, C.; Andersson, O.; Nyholm, L.; Bjorefors, F. *Angew. Chem., Int. Ed.* **2008**, *47*, 3034−3036.
(33) Chow, K. F.; Mavre, F.; Crooks, J. A.; Chang, B. Y.; Crooks, R. M. *J. Am. Chem. Soc.* **2009**, *131*, 8364−8365.
(34) Chow, K.-F.; Chang, B.-Y.; Zaccheo, B. A.; Mavré, F.; Crooks, R. M. *J. Am. Chem. Soc.* **2010**, *132*, 9228−9229.
(35) Chow, K. F.; Mavre, F.; Crooks, R. M. *J. Am. Chem. Soc.* **2008**, *130*, 7544−7545.
(36) Bard, A. J.; Fan, F. R. F.; Kwak, J.; Lev, O. *Anal. Chem.* **1989**, *61*, 132−138.
(37) Kwak, J.; Bard, A. J. *Anal. Chem.* **1989**, *61*, 1221−1227.
(38) Oleinick, A. I.; Battistel, D.; Daniele, S.; Svir, I.; Amatore, C. *Anal. Chem.* **2011**, *83*, 4887−4893.
(39) Horiuchi, T.; Niwa, O.; Morita, M.; Tabei, H. *J. Electroanal. Chem.* **1990**, *295*, 25−40.
(40) Horiuchi, T.; Niwa, O.; Morita, M.; Tabei, H. *J. Electrochem. Soc.* **1991**, *138*, 3549−3553.
(41) Tabei, H.; Horiuchi, T.; Niwa, O.; Morita, M. *J. Electroanal. Chem.* **1992**, *326*, 339−343.
(42) Oleinick, A.; Zhu, F.; Yan, J.; Mao, B.; Svir, I.; Amatore, C. *ChemPhysChem* **2013**, *14*, 1887−1898.
(43) Bond, A. M.; Luscombe, D.; Oldham, K. B.; Zoski, C. G. *J. Electroanal. Chem. Interfacial Electrochem.* **1988**, *249*, 1−14.
(44) Henry, C. S.; Fritsch, I. *J. Electrochem. Soc.* **1999**, *146*, 3367−3373.
(45) Wang, Y.; Limon-Petersen, J. G.; Compton, R. G. *J. Electroanal. Chem.* **2011**, *652*, 13−17.